4.1 MICROPHYSICAL IMPACTS ON IDEALIZED CLOUD-RESOLVING SIMULATIONS OF CIRRUS

Philip R.A. Brown[1] and David O'C Starr[2]
[1]Met Office, Farnborough, UK
[2]NASA Goddard Space Flight Center, Greenbelt, MD, U.S.A.

1.INTRODUCTION

The GEWEX Cloud System Study (GCSS, GEWEX is the Global Energy and Water Cycle Experiment) is a community activity aiming to promote development of improved cloud parameterizations for application in the large-scale atmospheric models used for climate research and numerical weather prediction. GCSS uses cloud-resolving models (CRMs); *i.e.* "process" models with sufficient spatial and temporal resolution to represent individual cloud elements but spanning a wide range of space and time scales to enable statistical analysis of simulated cloud systems (Randall et al. 2000).

The GCSS Working Group on cirrus clouds has conducted an intercomparison of CRM simulations of idealized cirrus cases. Key aims of these experiments were; (i) to determine what level of microphysical complexity is necessary to correctly represent the processes occurring in these clouds, (ii) to examine the interactions between microphysical processes, radiative heating and turbulence, and (iii) to examine the impact of key physical properties of the cirrus ice crystals, in particular their fall speed, on the evolution of the simulated clouds. This paper examines the simulation results in further detail.

2. MODEL DETAILS, INITIALIZATION AND FORCING OF SIMULATIONS

Some details of the CRMs participating in the study are shown in Table 1. Two sets of simulations are defined, referred to as "warm" and "cold" cirrus. with cloud top temperatures of –47C and –66C, respectively. Horizontally uniform profiles of temperature and relative humidity (RH) are defined, based on typical conditions for Spring/Fall 45 degN and Summer 30 degN for warm and cold cases, respectively. These have in common a 1km deep layer that is neutrally-stable w.r.t. ice-saturated pseudoadiabatic ascent. Within this layer, the initial RH w.r.t. ice reaches 120% over a depth of 0.5km. Forcing is by an imposed temperature tendency of approx. 1 K hr^{-1} to simulate ascent at 3 cm s^{-1}. After 4 hours, the forcing is switched off and the models run for a further 2 hours to simulate a dissipating cloud layer.

All models in the study had a fully-interactive radiation scheme capable of describing both long-wave and short-wave radiation although we chose to use only the long-wave scheme in each model, so as to represent a night-time cloud. Even with this simplification, different models may still be expected to have different treatments of the ice crystal effective radius and hence to produce different relationships between ice water path and optical depth.

A number of the 2- and 3-d CRMs use fully-explicit (multiple size-bin) microphysics. Aerosol properties in these models were the same as specified for the warm and cold cases of the Cirrus Parcel Model Comparison project (Lin et al. 2002).

Name	Type	Ice microphysics	Horiz./Vert Resol[tn]. [m]
CSU	3-d		100 / 50
PSU	2-d	Explicit, 25 bins	100 / 100
UKMO	3-d	2-class, dual-moment	100 / 100
DLR	2-d	1-class, dual-moment	100 / 100
LOA	2-d	3-class, single-moment	
ARC	2/3-d	Explicit, 25 bins	200 / 50
U. UTAH	2-d	Explicit	200 /200
GFDL	2-d	2-class, single-moment	100 /100
GSFC_L	2-d	Explicit, 25 bins	100 / 100
FRSGC	3-d	2-class, single moment	400 / 100
GSFC_S	2-d	1-class, single-moment	100 / 100
GSFC_T	3-d	3-class, dual moment	50 / 50

Table 1. Models used in Idealized Cirrus Model Comparison (ICMC).

3. RESULTS

3.1 Time evolution of integrated ice water path.

Fig.1 shows the evolution of the integrated ice water path (IWP). There is a spread of at least an order of magnitude in IWP and significant differences in the time of onset of cloud. The latter may be explained straightforwardly, by reference to the ice nucleation schemes active in each model. In models in which ice nucleation occurs by a heterogeneous process, this is commonly dependent on either the ice saturation ratio (Meyers et al. 1992) or temperature (Fletcher 1962). The initial supersaturation in the neutrally-stable layer ensures that cloud forms rapidly, within the first ten minutes of the simulation. Models with explicit microphysics typically represent nucleation by the homogeneous freezing of aerosol solution droplets. Model (Heymsfield and Sabin 1989) and observational (Heymsfield and Miloshevich 1993) studies show that for temperatures below –38C (ie. within the range of cloud formation temperatures for both warm and cold cases in the present study) nucleation occurs at a critical RH, dependent on temperature and vertical velocity. For these models, cloud formation only occurs once the combination of

[1]*Corresponding author address:*
Philip R.A. Brown, Met Office, Y46 Building, Cody Technology Park, Farnborough, GU14 0LX, UK.
e-mail *Phil.Brown@metoffice.com*

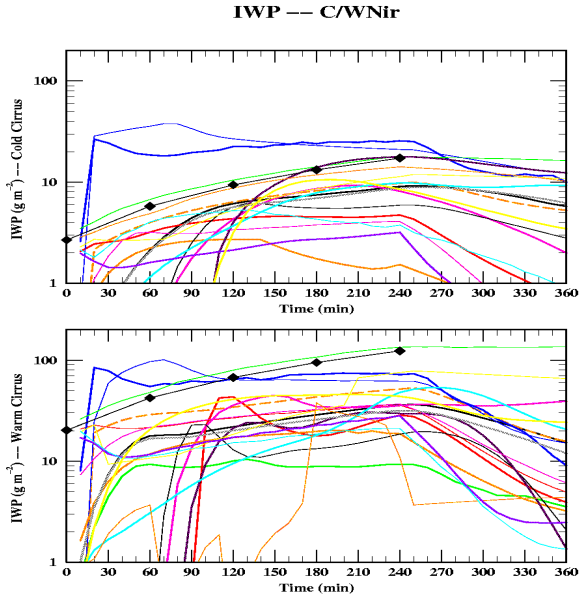

Figure 1. Time evolution of integrated ice water path (IWP) for cold (upper) and warm (lower) cases. The line with symbols shows potential IWP as defined in the text.

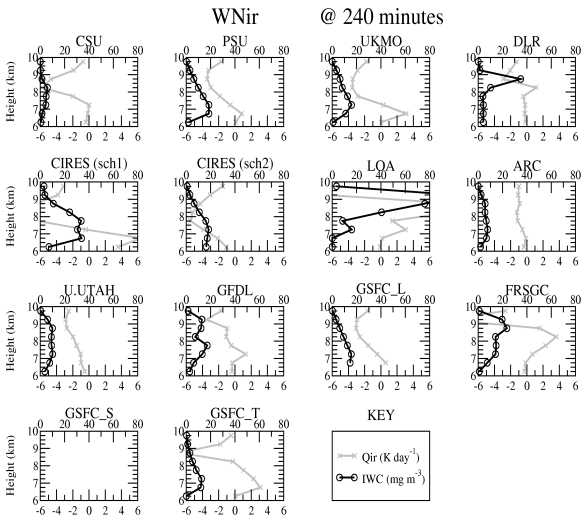

Figure 2. Vertical profiles of ice water content (IWC) in warm simulations at 4hr (black) with longwave heating rates (grey).

large-scale cooling and the cooling in updraft circulations generated by the perturbation temperature field enables the critical RH to be achieved. One CRM with bulk microphysics (UKMO) simulates homogeneous freezing by allowing ice nucleation when water saturation is achieved on a grid point. This is a reasonable approximation for cloud formation temperatures close to –40C, but the need to achieve water saturation ensures that this model is the last to form cloud. Between 3 and 4 hours, the IWP of most models varies only slowly, generally showing a slow increase. We take this period as representing the models' quasi-equilibrium response to the forcing.

Fig.2 presents vertical profiles of the domain-averaged IWC for each model. These show that the CRMs can be grouped into one of three types of behaviour. These are illustrated below and the

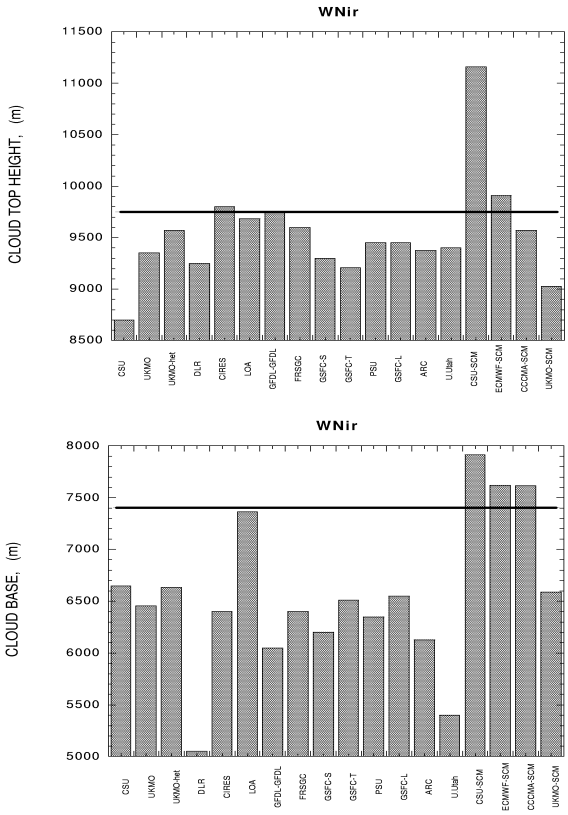

Figure 3. Cloud top (upper) and base (lower) altitudes at 4hr in standard warm cases. Horizontal lines show the potential values defined in the text.

terminology used subsequently throughout this paper. The first group have IWC profiles which increase steadily from cloud-top to cloud base (Fig. 2 UKMO) and are referred to subsequently as "bottom-peaked". The second (and smaller) group have IWC profiles that have a maximum near the cloud top and are referred to as "top-peaked" (Fig. 2 LOA). The third group have a more obvious two-layer IWC profile and are referred to as such (Fig. 2 GFDL). This division is somewhat arbitrary but facilitates subsequent discussions.

3.2 Time evolution of cloud boundaries

The models are initialized with common temperature and water vapour profiles and forced only by large-scale temperature changes. Hence, it is expected that the cloud top and base will respond principally to increases in the mean RH profiles due to cooling with the water vapour profile conserved, and re-distribution of water due to the presence of the cloud, caused by ice fallout below the cloud layer and upward mixing of water vapour by turbulence within the cloud.

The first of these effects may be calculated by taking the initial temperature profile, cooling it in response to the large-scale forcing and then calculating its saturation mixing ratio. We may then calculate "potential cloud top/base" altitudes as the upper and lower altitudes for which the initial mixing ratio profile exceeds the saturation value.

Fig.3 shows the cloud base and top altitudes for standard warm simulations at 4 hours. Also shown are

the potential cloud top and base altitudes. For the majority of the CRMs, the cloud top does not exceed the potential cloud top. Since some of models allow ice nucleation whenever ice saturation is exceeded, this implies that ice fallout plays a major role in removing ice mass from the cloud top region and reducing the cloud top altitude from its potential upper limit.

The UKMO model allows nucleation only when water saturation is achieved. However, in this run the cloud top altitude exceeds that of the layer which will have been brought to water saturation by the forcing. This implies that there has been upward turbulent transport of water vapour. Examination of the water budget terms for this simulation confirms that this is the case.

From the potential cloud top and base, we may calculate a potential IWC and vertically integrated IWP. As this is derived simply from the excess mixing ratio over saturation, it represents the IWC that would be obtained in the absence of any ice fallout or mixing. It ignores any additional net cooling of the cloud layer due to radiative processes or heating due to the release of latent heat, but does give some guidance as to the upper limit of IWC and IWP that are expected in each case. At times of 0, 2 and 4 hours, the potential IWP has values of 20.2, 67.5 and 123.1 gm^{-2}, respectively. The profile of potential IWC has a peak which is closer to the base of the layer, similar to the "bottom-peaked" IWC profiles shown in Fig.3, a function simply of the temperature dependence of the saturation mixing ratio. Hence, any model in which the peak IWC occurs at a higher altitude than that of the peak potential IWC has significant upwards transport of ice, such that the mean ice fall speed in the updraught cores is less than the updraught strength.

The majority of models have cloud bases which are below the potential cloud base, so we expect that they will have IWP below the potential IWP since cloud ice must have precipitated and evaporated into the unsaturated region below the potential cloud base. The change, ΔIWP, in IWP due to evaporation of ice below the potential cloud base may be calculated, taking into account the cooling produced by evaporation.

Values of potential IWP and ΔIWP for various actual cloudbase altitudes in the warm and cold cases are given at 4 hours in Table 2. Values of potential IWP at hourly intervals are also plotted in Fig.1. For the warm case, the majority of models have actual cloud bases between 6.2 and 6.6 km suggesting that the range of IWP at 4 hr should lie somewhere between about 5 and 72 gm-2. This is in good general agreement with the results shown in Fig.1.

If the potential IWP values in Table 2 are compared with the time-series shown in Fig.1, it may immediately be seen that one model, LOA, generates IWP values close to the potential IWP with cloud top and base which are close to the potential values. Its IWC profile is, however, one that is "top-peaked" (see Fig.2). This model assumes that cloud ice has zero fall speed. Since no ice is lost from the cloud layer by precipitation, the top-peaked profile is maintained by the upward turbulent transport of ice and vapour producing IWC profiles that are reminiscent of the LWC profiles found in stratocumulus cloud.

We do not expect perfect agreement between the models' cloudbase and residual IWP. IWP is reduced by the entrainment of sub-saturated air from above cloud-top. Additionally, some models will be able to maintain a layer near cloudbase in which ice exists in unsaturated air. This is more likely in those models that distinguish between small pristine ice crystals and larger particles such as aggregates. The latter, having higher fall velocities, will penetrate further in unsaturated air before evaporating completely. From such a model, we would diagnose a lower cloudbase and a higher IWP than that given by the simple analysis above. Significant penetration of precipitating ice into unsaturated air is indicated by those IWC profiles which do not have a sharp cutoff at cloudbase but decline more slowly to zero. For cold case simulations, a number of models have a cloudbase below 11.4 km but IWP above the lowest residual value in Table 2. This suggests that these models have significant penetration of falling ice into unsaturated air.

WARM CASE

Potential cloud base [km]	Potential IWP [g m-2]	
7.41	123.1	
Actual cloud base [km]	**ΔIWP [g m-2]**	**Residual IWP [g m-2]**
7.0	9.1	114.8
6.8	26.2	97.7
6.6	51.0	72.9
6.4	79.6	44.3
6.2	118.7	5.2
6.0	164.0	

COLD CASE

Potential cloud base [km]	Potential IWP [g m-2]	
12.34	17.3	
Actual cloud base [km]	**ΔIWP [g m-2]**	**Residual IWP [g m-2]**
12.0	1.8	15.5
11.7	6.7	10.6
11.4	14.5	2.8
11.1	26.1	
10.8	41.9	
10.5	61.4	

Table 2 Potential IWP assumes conservation of the initial water vapour profile and condensation of any local excess over saturation w.r.t. ice. ΔIWP is the IWP deficit required to saturate w.r.t. ice the region between potential cloud base and the given altitude. Residual IWP is the difference between potential IWP and ΔIWP.

3.3 Impact of fixed ice fall speeds

In models with prognostic ice number (either bulk or explicit schemes), higher concentrations give smaller mean particle sizes, and hence smaller mean fall speeds, for a given IWC. A fixed fall speed for ice removes feedbacks between this and the nucleation processes. It also removes differences between

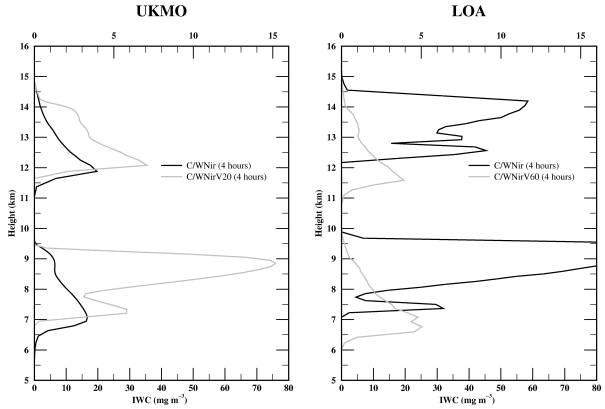

Figure 4. IWC profiles at 4hr with (Left) UKMO standard (black) and fixed fall speed 20 cm s^{-1} (grey), and (Right) LOA standard (black) and fixed 60 cm s^{-1} (grey). Upper curves on each plot are Cold cases whilst lower curves are Warm.

Model	V = 20 cm s^{-1}		V = 60 cm s^{-1}	
	Cold	Warm	Cold	Warm
PSU	1.2	2.5	0.6	1.0
UKMO	2.0	2.8	0.7	0.8
DLR	2.7	3.0	0.6	1.2
LOA	0.7	0.8	0.3	0.3
GFDL	1.7	1.5	1.0	1.0
GSFC_L	1.2	2.3	0.5	1.0
GSFC_S			4.7	1.0
GSFC_T	2.0	4.8	1.4	2.3

Table 3 The ratio of IWP in fixed-fall speed runs to IWP in standard model, after 4 hours.

models due to their choice of parameter values describing the mass and fall speed of a single crystal.

The impact of running a number of the models with fixed fall speeds is illustrated in Table 3, giving the ratio of IWP for fixed fall speed to that in the standard run, for the two values of fall speed that were used (20 and 60 cm s^{-1}). The value of 20 cm s^{-1} always acts to increase the IWP, except for the LOA model which has as standard zero fall speed for cloud ice.

Fig.4 shows vertical profiles of IWC at 4hr in both Cold and Warm cases for the models LOA and UKMO. For UKMO, the effect of using a fixed 20 cm s^{-1} fall speed is to alter the shape of the IWC profile from bottom- to top-peaked. This in turn allows a radiative heating gradient to be maintained across the neutrally-stable layer in both warm and cold cases, resulting in greatly-increased values of the mean vertical velocity standard deviation, which exceed the fixed ice fall speed. The models show a characteristic minimum in IWC around 8km altitude in the Warm case and 13km in the Cold case. This is the base of the neutrally-stable layer and so is the lowest level in the cloud to be affected by radiatively driven turbulence, ice evaporating in the downdrafts.

The LOA model is converted from a top-peaked IWC profile in the control run to a bottom-peaked profile with ice fall speed of 60 cm s^{-1}. This value exceeds the mean W_{RMS} and so ice accumulates at the base of the cloud layer, giving a similar structure to the UKMO model, which generates mean fall speeds closer to 60 cm s^{-1} throughout the run.

4. CONCLUSIONS

The comparison of CRM simulation in the ICMC shows a wide degree of difference in simple properties of the cirrus cloud system, such as IWP, cloud base and top altitudes etc. We can, however, make links between key physical processes:

i) Where sufficient IWC is retained in a layer of near-neutral static stability, the vertical gradient of radiative heating acts to generate turbulent motions in the layer, increasing its horizontal inhomogeneity.

ii) The mean ice fall speed is the key determinant of the IWC retained in the cloud layer or evaporated in the sub-saturated air below. Fixed fall speeds promote convergence in vertical structure generated by models with either explicit or bulk microphysics.

iii) Clouds in a statically stable environment have similar properties such as IWP, base and top, but the suppression of turbulence reduces spatial structure.

iv) Models that distinguish between large and small ice (by means of either size bins or large-particle categories in bulk schemes) have greater depth scales for the evaporation of ice in subsaturated air.

ACKNOWLEDGEMENTS

The following contributed to the results described in this paper: Angela Benedetti, Matt Boehm, Klaus Gierens, Vincent Giraud, Eric Girard, Eric Jensen, Vitaly Khvorostyanov, Martin Koehler, Ruei-Fong Lin, Ken-Ichi Maruyama, Wei-Kuo Tao and Yansen Wang. Assistance with the data analysis and preparation of figures was provided by Andrew Lare.

REFERENCES

Lin, R-F, D.O'C.Starr, P.J.DeMott, R.Cotton, E.Jensen, B.Kaercher and X.Liu. (2002) Cirrus Parcel Model Comparison Project: Phase 2. *This conference*

Fletcher, N.H. (1962) The physics of rainclouds. Cambridge University Press, London

Heymsfield, A.J. and L.M.Miloshevich (1993) Homogeneous ice nucleation and supercooled liquid water in orographic wave clouds. J.Atmos.Sci., **50**, pp2335-2353.

Heymsfield, A.J. and R.M.Sabin (1989) Cirrus crystal nucleation by homogeneous freezing of solution droplets. J.Atmos.Sci., **46**, pp2252-2264.

Meyers,M.P., P.J.DeMott and W.R.Cotton (1992) New primary ice nucleation parametrizatons in an explicit cloud model. J.Appl.Met., **31**, pp708-721.

Randall,D.A., J.Curry, P.Duynkerke, S.Krueger, M.Miller, M.Moncrieff, B.Ryan, D.Starr and W.Rossow. (2000) The second GEWEX Cloud System Study science and implementation plan. IGPOReport 34.